

# Low cycle fatigue of an austenitic TRIP steel under various biaxial-planar stress states

S. Ackermann, D. Kulawinski, S. Henkel, H. Biermann

Institute of Materials Engineering, Technische Universität Bergakademie Freiberg,  
Gustav-Zeuner-Str. 5, 09599 Freiberg, Germany  
E-mail: Stephanie.Ackermann@iwt.tu-freiberg.de

**ABSTRACT.** *Biaxial experiments with cruciform specimens can be used to determine the influence of the biaxial stress states on the material behavior, but are rare in literature. In the present study the cyclic deformation and fatigue behavior of a austenitic CrMnNi TRIP steel was investigated under biaxial out-of-phase and biaxial in-phase loading with different phase angles  $\Phi$  as well as uniaxial loading. The biaxial experiments were performed by using a servohydraulic tension-compression test rig and cruciform specimens. The results show similar fatigue lives under out-of-phase loading in comparison to in-phase loading with  $\Phi = 0^\circ$  and much higher fatigue lives under  $180^\circ$  in-phase loading than under all other stress states. The reason was not given by the martensitic phase transformation of the steel which causes secondary hardening during cyclic deformation. No significant dependence of the fatigue life on the martensite formation and the secondary hardening were found. Moreover, it seems that there is no linear correlation between the phase angle  $\Phi$  and the martensite formation as well as the secondary hardening. As possible explanations for the fatigue lives under biaxial in-phase and out-of-phase loading the microcrack propagation directions and the hydrostatic stress component were discussed.*

## INTRODUCTION

In the Collaborative Research Centre 799 „TRIP-Matrix-Composite” an high alloyed austenitic cast CrMnNi steel was developed. The metastable steel shows a deformation-induced transformation from austenite into  $\varepsilon$ - and/or  $\alpha'$ -martensite. This causes additional strength and ductility, called TRIP effect (TRansformation Induced Plasticity) and a secondary hardening under cyclic loading [1, 2, 3]. The martensitic transformation is accompanied by volume changes which result in additional stresses. Thus, it is suggested that the stress state has an influence on the martensite evolution. This was extensively studied under static loading and described by different parameters, e.g. triaxiality [4].

Cyclic investigations on the martensite transformation behavior at different biaxial-planar stress states are missing, but results on the cyclic deformation and fatigue behavior are available. Pascoe and de Villiers [5] performed different biaxial in-phase

experiments for two steels. Out-of-phase fatigue data were presented by Ogata and Takahashi [6] for a 316FR stainless steel at 550°C as well as Henkel et al. [7] for copper and alpha-brass at room temperature. Both reported a reduction of the fatigue lives under out-of-phase loading compared to in-phase loading.

In the present study cyclic biaxial-planar in-phase (equibiaxial, shear) as well as out-of-phase experiments with phase angles  $\Phi$  of 22.5°, 45° and 135° were performed. The purpose is to investigate the effect of biaxial stress states on the cyclic deformation, martensitic transformation and fatigue behavior of an austenitic CrMnNi TRIP steel.

## EXPERIMENTAL DETAILS

### *Material*

The studied material is a metastable austenitic stainless steel with 16 % Cr, 6 % Mn and 6 % Ni which was casted in plates of several batches. Table 1 gives the chemical composition. During deformation the steel exhibits martensitic transformation causing a secondary hardening during cyclic deformation [1, 3, 8]. The microstructure of the TRIP steel is dendritic and mainly austenitic with less than 3 %  $\delta$ -ferrite due to solution heat treatment (1050 °C, 30 min, vacuum) and quenching (N<sub>2</sub> atmosphere). The grains are coarse and some extend over the whole specimen thickness of 1.6 mm in the gauge area affecting the deformation behavior.

Table 1. Chemical composition of the studied CrMnNi TRIP steel batches

	C	Cr	Mn	Ni	Si	Al	N	Fe
wt.%	0.04 – 0.06	15.3 – 16.3	5.4 – 6.5	5.8 – 7.3	0.8 – 1.0	0.07 – 0.18	0.05 – 0.11	bal.

### *Biaxial-planar testing*

Biaxial-planar fatigue tests were carried out on a servohydraulic tension-compression test rig with four cylinders of 250 kN (Instron 8800), see Fig. 1a. The uniaxial reference tests were carried out for the same steel on a 250 kN servohydraulic testing system (MTS Landmark) at a constant strain rate of 0.004 s<sup>-1</sup> [1]. The biaxial specimens have a cruciform geometry (Fig. 1b) and a planar circular centre ( $\varnothing$  16 mm) of reduced thickness (1.6 mm) to get the highest stresses in the gauge area [5]. Both sample surfaces were mechanically polished. On one side a biaxial orthogonal extensometer (Sandner) was applied to measure total strains in the planar centre. A ferrite sensor (Fischer) at the other side measured in situ the  $\alpha'$ -martensite volume fraction.

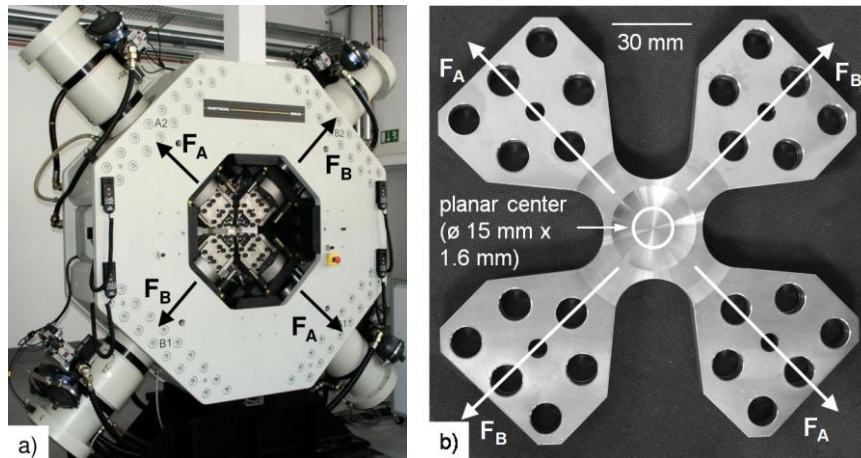


Figure 1. a) Servohydraulic biaxial planar test rig and b) cruciform specimen

### *Cyclic loading path*

Biaxial cyclic tests were performed at von Mises equivalent strain amplitudes  $\varepsilon_{eq,a}$  of 0.49 – 0.53 % with strain rates of 0.003 – 0.005 s<sup>-1</sup> under variation of the phase angle  $\Phi$  between the loading axes A and B. A triangular total strain-time function was applied in the axes A and B with the same frequency and total strain amplitude, see Fig. 2. Phase angles  $\Phi$  of 0° (equibiaxial) and 180° (shear) are in-phase loading cases and  $\Phi = 22.5^\circ$ , 45° and 135° are out-of-phase loading cases. During a cycle the strain ratio of the total strain in axis A to the total strain in axis B is constant under in-phase loading ( $\Phi = 0^\circ$ , 180°) and vary under out-of-phase loading (22.5°, 45°, 135°).

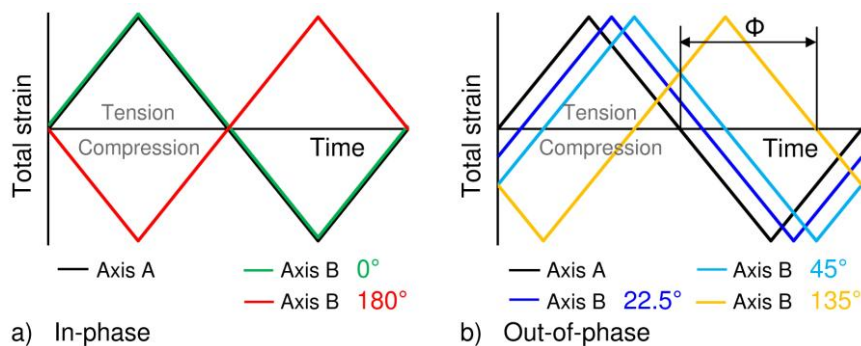


Figure 2. Triangular total strain-angle function in each axis for different phase angles  $\Phi$  a) in-phase loading ( $\Phi = 0^\circ$ , 180°) and b) out-of-phase loading ( $\Phi = 22.5^\circ$ , 45°, 135°)

The various investigated phase angles cause different strain paths  $\varepsilon_{t,A}-\varepsilon_{t,B}$  during a cycle for equivalent strain amplitudes of about 0.50 % according to distortion energy hypothesis (DEH), see Fig. 3. Under equibiaxial and shear loading (in-phase) the loading paths are straight lines inclined under 45° to the axes  $\varepsilon_1$  and  $\varepsilon_2$  and

perpendicular to each other. Thus, the deformation and back deformation during a cycle is proportional and runs through the origin. With increasing phase angle from  $0^\circ$  to  $180^\circ$  the loading path becomes a rectangle with increasing width and decreasing length. The rectangles are symmetric to the  $45^\circ$  lines of  $\Phi = 0^\circ$  and  $180^\circ$ .

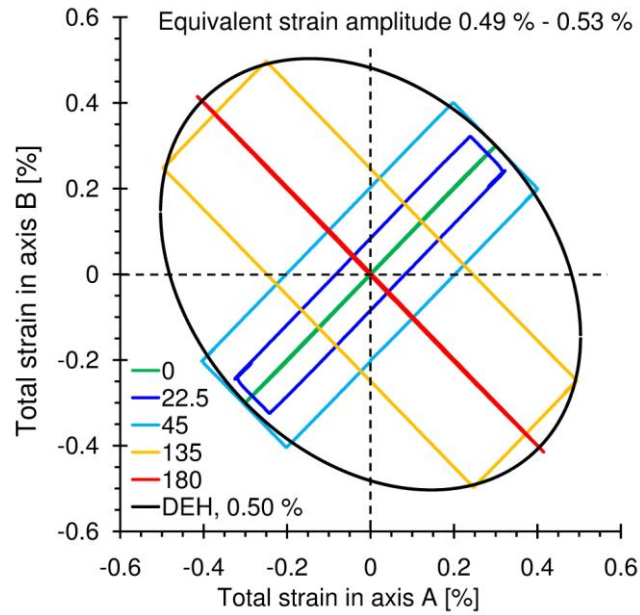


Figure 3. Strain paths during a cycle for in-phase ( $\Phi = 0^\circ, 180^\circ$ ) and out-of-phase loading ( $\Phi = 22.5^\circ, 45^\circ, 135^\circ$ ) at  $\epsilon_{eq,a} = 0.49 - 0.53 \%$

### ***Stress and strain calculation***

The stress calculation is based on the elastic unloading method instead of  $\sigma = F/A$  because the cross sectional area  $A$  of the cruciform specimen is undefined. In in-phase tests the simultaneous elastic unloading of both axes at the load reversals during a cycle are used to determine the elastic strains in each axis [8]. In out-of-phase tests the load reversal of axis B is shifted to a later time, thus an additional partial load relief has to be inserted. The von Mises criterion was adopted to estimate the equivalent stress amplitude  $\sigma_{eq,a}$  and the equivalent strain amplitude  $\epsilon_{eq,a}$ . For details see [8].

## **RESULTS AND DISCUSSION**

### ***Cyclic deformation and martensitic transformation***

Figure 4 presents the cyclic deformation curves and the  $\alpha'$ -martensite evolution for the uniaxial and the biaxial in-phase ( $\Phi = 0^\circ$ ) and out-of-phase ( $\Phi = 22.5^\circ, 45^\circ$  and  $135^\circ$ )

tests at equivalent strain amplitudes  $\varepsilon_{\text{eq,a}}$  of 0.49 – 0.52 %. The values at half fatigue life were marked by squares. The 45° out-of-phase test was stopped before failure occurred. The cyclic deformation curves show a pronounced secondary cyclic hardening after stress saturation. This is mainly caused by martensitic phase transformation [1, 3, 8], see Fig. 4. Additional hardening, as known from out-of-phase tension-torsion tests [9], is not induced due to fixed perpendicular loading axes.

The secondary hardening rate depends on the martensite formation rate. The highest rates were observed in the uniaxial test. Under out-of-phase loading both rates were lower than under in-phase loading, but the onsets are shifted to lower numbers of cycles. At failure the  $\alpha'$ -phase contents and the stresses of the fatigue tests differ widely. For the biaxial stress states martensite volume fractions of 19 % ( $\Phi = 22.5^\circ$ ) to 46 % ( $\Phi = 135^\circ$ ) and equivalent stress amplitudes of 290 MPa ( $\Phi = 22.5^\circ$ ) to 410 MPa ( $\Phi = 45^\circ$ ) were determined. The highest values were observed under uniaxial loading (55 % and 520 MPa). However, the fatigue lives are similar for the investigated loading cases, see Figure 4. It seems that there is no linear dependence between the phase angle  $\Phi$  and the evolutions of the  $\alpha'$ -martensite content and the stress amplitude. Moreover, it is necessary to take into account the orientation of the large grains, varying chemical composition and material heterogeneities.

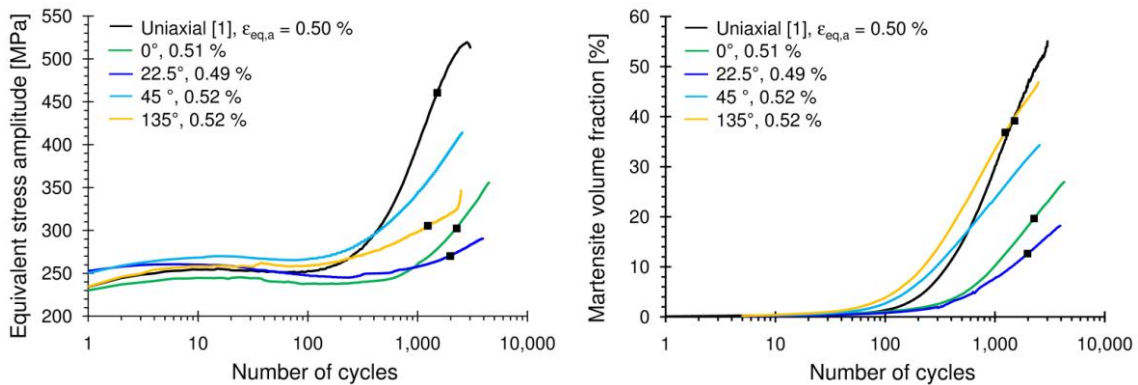


Figure 4. a) Cyclic deformation curves and b)  $\alpha'$ -martensite evolution under uniaxial [1] and biaxial loading with  $\Phi = 0^\circ, 22.5^\circ, 45^\circ$  and  $135^\circ$  at  $\varepsilon_{\text{eq,a}} = 0.49 - 0.52 \%$

### ***Fatigue live***

The fatigue lives versus the strain amplitudes of the in-phase and out-of-phase cyclic tests are presented in Fig. 5a. The number of cycles to failure was determined at a load decrease of 15 % in the uniaxial test and at a reduction of specimen stiffness of 5 % in the biaxial tests by using the elastic unloading method. Both reflect the damage evolution until one crack has a technically measurable length. The Basquin and Manson-Coffin relationships were used to quantify the lifetimes. Table 2 gives the corresponding parameters fatigue strength coefficient  $\sigma_f'$  and exponent  $b$  (Basquin) as well as fatigue ductility coefficient  $\varepsilon_f'$  and exponent  $c$  (Manson-Coffin), respectively.

Table 2. Parameters of Basquin ( $\sigma_f'$ ,  $b$ ) and Manson-Coffin ( $\epsilon_f'$ ,  $c$ ) for the uniaxial and biaxial stress states

Stress state	$\sigma_f'$	$b$	$\epsilon_f'$	$c$
Uniaxial	2144	-0.18	0.09	-0.45
$\Phi = 0^\circ$ biaxial in-phase (equibiaxial)	1123	-0.14	0.33	-0.53
$\Phi = 22.5^\circ$ out-of-phase	667	-0.10	0.15	-0.43
$\Phi = 180^\circ$ biaxial in-phase (shear)	952	-0.09	0.06	-0.27

As reported in [8] the fatigue lives for  $\Phi = 0^\circ$  in-phase loading were up to 2.5 times higher than those of the uniaxial tests, contrary to [5], although higher hydrostatic stress ( $\sigma^H = 2/3 \sigma_1$ ) was available to open fatigue cracks than under uniaxial loading ( $\sigma^H = 1/3 \sigma_1$ ). The lowest fatigue lifetimes were observed under uniaxial loading and the highest under  $\Phi = 180^\circ$  in-phase loading. Thus, the  $\Phi = 180^\circ$  loading case was the least dangerous biaxial stress state due to zero hydrostatic stress ( $\sigma^H = 0$ ). Ogata and Takahashi [6] observed the same sequential arrangement of fatigue lives for AISI 316 FR at  $550^\circ\text{C}$ : uniaxial –  $0^\circ$  –  $180^\circ$ . Thus, the von Mises criterion is not appropriate to correlate biaxial fatigue lifetimes. Probably, also the effect of the hydrostatic stress component has to be considered.

The much higher fatigue lives under  $180^\circ$  in-phase loading compared to  $0^\circ$  in-phase loading can be explained by crack growth behavior according to [10]. Therefore, cracks on the specimen surfaces were investigated in an electron beam universal system (pro beam, K26-15/80) which was used due to the dimensions of the cruciform specimens.

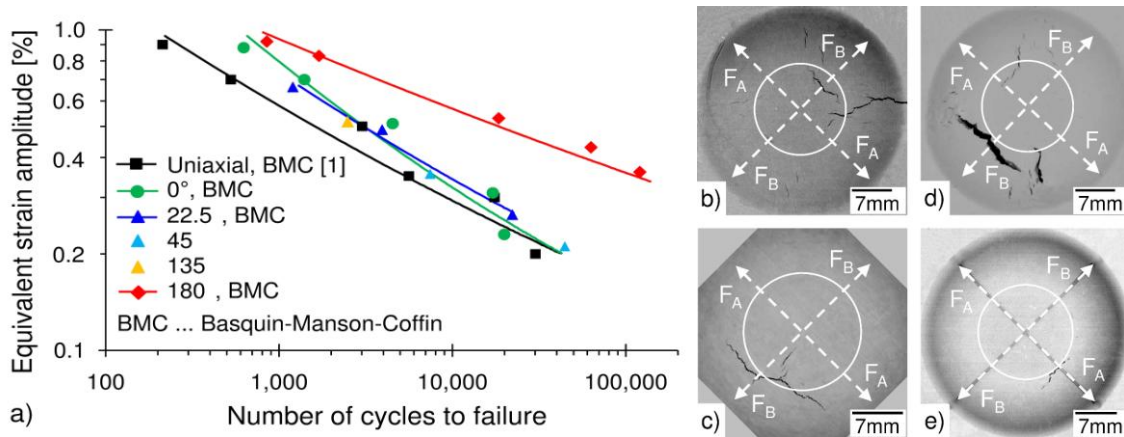


Figure 5. Fatigue lifetimes vs. equivalent strain amplitude under uniaxial [1] and biaxial loading ( $\Phi = 0^\circ, 22.5^\circ, 45^\circ, 135^\circ$  and  $180^\circ$ ); surface images obtained by an electron beam universal system after biaxial loading at b)  $\Phi = 0^\circ$ ,  $\epsilon_{eq,a} = 0.51\%$ ,  $N_f = 4520$ , c)  $\Phi = 180^\circ$ ,  $\epsilon_{eq,a} = 0.53\%$ ,  $N_f = 63000$ , d)  $\Phi = 22.5^\circ$ ,  $\epsilon_{eq,a} = 0.49\%$ ,  $N_f = 3931$  and e)  $\Phi = 135^\circ$ ,  $\epsilon_{eq,a} = 0.52\%$ ,  $N_f = 2487$

Figure 5b shows a number of surface cracks after  $0^\circ$  in-phase loading with random orientation to the principal strain axes which was also reported in [11]. Under in-phase loading with  $\Phi = 180^\circ$  the direction of the cracks were parallel to the loading axes, see Figure 5c. This investigations are in accordance with the theory of Brown and Miller [10]. Cracks under  $0^\circ$  in-phase loading propagate through the specimen thickness, thus the fatigue life is reduced in comparison to cracks under  $180^\circ$  in-phase loading which grow along the surface.

The fatigue lives under the studied out-of-phase loading conditions ( $\Phi = 22.5^\circ, 45^\circ$  and  $135^\circ$ ) are in the scatter band of the in-phase tests with  $\Phi = 0^\circ$  (equibiaxial). This result is contrary to the reports for 316FR stainless steel at  $550^\circ\text{C}$  [6] as well as for copper and alpha-brass at room temperature [7]. The phase angle seems to have no significant influence on the fatigue lifetime, except  $\Phi = 180^\circ$  (shear). Probably, this can be understood by comparing the equivalent stress amplitude and the hydrostatic stress amplitude  $\sigma^H = (\sigma^H_{\text{tension}} - \sigma^H_{\text{compression}}) / 2$  of the different out-of-phase tests in the saturation range (after 100 cycles) at similar equivalent strain amplitudes of 0.49 – 0.52 %. As expected, the equivalent stress amplitudes were in a narrow range between 237 MPa ( $\Phi = 0^\circ$ ) and 267 MPa ( $\Phi = 45^\circ$ ), see Figure 4a. But also the hydrostatic stress amplitudes were nearly the same and range between 159 MPa ( $\Phi = 0^\circ$ ) and 167 MPa ( $\Phi = 135^\circ$ ). This led us to the hypothesis that the normal stresses available to open fatigue cracks were similar under out-of-phase loading and in-phase loading with  $\Phi = 0^\circ$ . Thus, the damage evolution and the fatigue lives were similar.

Therefore, the surface cracks were investigated after failure, see Figure 5b – 5e, but did not confirm clearly confirm our hypothesis. Cracks under  $22.5^\circ$  loading were similar oriented as under  $0^\circ$  loading, perpendicular and  $45^\circ$  to one loading axis. Under  $135^\circ$  loading only one crack perpendicular to a loading axis was observed. Further investigations in the scanning electron microscope are necessary.

## CONCLUSIONS

Biaxial-planar in-phase ( $\Phi = 0^\circ, 180^\circ$ ) and out-of-phase ( $\Phi = 22.5^\circ, 45^\circ, 135^\circ$ ) tests with cruciform specimens were performed to study the fatigue behavior of a CrMnNi TRIP steel.

Contrary to the literature [6, 7], the fatigue lives under out-of-phase loading were similar as under in-phase loading with  $\Phi = 0$  (equibiaxial). For in-phase loading with  $\Phi = 180^\circ$  (shear) much higher fatigue lives were observed than for all other stress states. Therefore, the distortion energy criterion is not appropriate to correlate biaxial fatigue lives.

An explanation for the biaxial fatigue lives was not be given by the martensitic phase transformation of the steel which causes a pronounced secondary hardening. The secondary hardening rate was directly related to the martensite formation rate, but no significant correlation to the fatigue life was found. Both the secondary hardening rate and the martensite formation rate differ widely in the biaxial tests and the highest rates were observed under uniaxial loading. Moreover, it seems that there is no linear

dependence between the phase angle  $\Phi$  and the evolutions of the  $\alpha'$ -martensite volume fraction and the equivalent stress amplitude.

The fatigue lives under biaxial in-phase loading and out-of-phase biaxial loading were discussed by taking into account the microcrack propagation directions and the hydrostatic stress component and its effect on the crack behavior [10, 11].

## ACKNOWLEDGMENT

The authors acknowledge the German Research Foundation for supporting the Collaborative Research Centre 799 "TRIP-Matrix-Composite". We thank Mr. Glage for the uniaxial fatigue data and Mr. R uthrich for taking the surface crack images.

## REFERENCES

1. Glage, A., Weidner, A., Biermann, H. (2011) *Steel Res. Int.* **82** (9), 1040–1047.
2. Jahn, A., Kovalev, A., Wei , A., Wolf, S., Kr ger, L., Scheller, P.R. (2011) *Steel Res. Int.* **82** (9), 39–44.
3. Bayerlein, M., Christ, H.-J., Mughrabi, H. (1989) *Mater. Sci. Eng.* **114**, L11–L16.
4. Beese, A.M., Mohr, D. (2011) *Acta Mater.* **59** (7), 2589–2600.
5. Pascoe, K.J., de Villiers, J.W.R. (1967) *J. Strain Anal. Eng. Des.* **2** (2), 117–126.
6. Ogata, T., Takahashi, Y. (1999) In: *Multiaxial fatigue and fracture* Macha, pp. 101–114, E., Bedkowski, W., Lagoda, T. (Ed.), Elsevier.
7. Henkel, S., Fischer, H., Balogh, L., Ungar, T., Biermann, H. (2010) *J. Phys.* **240**, 012042.
8. Kulawinski, D., Ackermann, S., Glage, A., Henkel, S., Biermann, H. (2011) *Steel Res. Int.* **82** 9, 1141–1148.
9. Itoh, T., Sakane, M., Ohnami, M., Socie, D. (1995) *J. Eng. Mater. Technol.* **117**, 285–292.
10. Brown, M., Miller, K. (1973) *Proc. Inst. Mech. Eng.* **187**, 745–755.
11. Parsons, M.W., Pascoe, K.J. (1976) *Mater. Sci. Eng.* **22**, 31–50.